Available online at www.sciencedirect.com
SCIENCE DIRECT
Journal of Magnetic Resonance 180 (2006) 110–117
JMR Journal of Magnetic Resonance
www.elsevier.com/locate/jmr

Improvement of the inverse-gated-decoupling sequence for a faster quantitative analysis of various samples by ^{13}C NMR spectroscopy

Patrick Giraudeau, Evelyne Baguet *

Laboratoire d'Analyse Isotopique et Electrochimique de Métabolismes, UMR CNRS 6006, Université de Nantes, B.P. 92208, 2 rue de la Houssinière, F-44322 Nantes Cedex 03, France

Received 28 October 2005; revised 25 January 2006
Available online 20 February 2006

Abstract

The inverse-gated-decoupling sequence enables quantitative ^{1}H decoupled ^{13}C spectra to be obtained. We modified this sequence so as to obtain the same result in less time for molecules containing carbons with various relaxation properties. For that, we determined the optimal ^{13}C longitudinal-magnetization initial value for a faster relaxation while ^{1}H decoupler is stopped. This value can be calculated precisely via the nuclear Overhauser effects, the longitudinal relaxation times, together with the determination of the relaxation rate constants of carbons while ^{1}H are out of equilibrium. A supplementary delay of ^{1}H decoupling and/or a series of selective pulses applied at the beginning of the recovery delay allow an acceleration of ^{13}C longitudinal relaxation. We applied this method to the molecule of vanillin. The simultaneous quantification of all carbons was carried out with a recovery delay divided by two compared to the usual sequence.

Keywords: Inverse-gated decoupling; Quantitative NMR; ^{13}C spectroscopy; Dipolar relaxation; Vanillin

1. Introduction

^{13}C NMR spectroscopy offers a high potential for the quantitative analysis of complex mixtures, due to the broad spectral range and, usually, an absence of interference between peaks. Various quantitative applications of this method have been performed, such as food analysis [1], authentication of natural products [2] or metabolites quantification [3].

It suffers, however, from poor sensitivity due to the low abundance and small magnetic moment of the ^{13}C nucleus. This sensitivity is further diminished if the conditions of quantitative NMR—inverse-gated-decoupling procedure with decoupling on during the acquisition only [4] and a recovery delay, from the end of the acquisition to the next read pulse, between 5- and 10-times the longest spin–lattice relaxation time [5–7]—are employed. In fact, the use of these acquisition conditions may lead to unacceptably long accumulation times to obtain a spectrum with an acceptable signal/noise ratio for a solute in small concentration.

An alternative is to add a paramagnetic relaxation reagent [8], such as triacetylacetonatochromium (III) $Cr(AcAc)_3$, which shortens the relaxation times. The unwanted side-effect of adding $Cr(AcAc)_3$ is that it leads to line broadening. Furthermore, it may not always be desirable to add a paramagnetic relaxation reagent to a biological sample, as this could modify it. Another method is to detect the signal in non-quantitative conditions for comparing concentrations of molecules with similar relaxation properties [9]. It may only be employed to study a mixture of alike molecules. The DEPT sequence [10], when adapted [11] can also be applied for quantification, but only to compare alike carbons which resonate in a small spectral range.

Finally, when a precise ^{13}C NMR quantitative spectrum is needed for a sample with different carbons in a 200 ppm

* Corresponding author. Fax. +330 2 51 12 57 12.
E-mail address: Evelyne.Baguet@univ-nantes.fr (E. Baguet).

1090-7807/$ - see front matter
doi:10.1016/j.jmr.2006.01.015

range, the inverse-gated-decoupling sequence is still employed with a recovery delay of about seven times the largest T_1, for the different carbons of interest [2].

In a recent article [12], we described an improvement of the inverse-gated-decoupling sequence to obtain quantitative results in less time, by adding a supplementary decoupling delay and a pulse at the beginning of the recovery delay. We showed that with an adequate adjustment of these parameters, ^{13}C longitudinal magnetization goes back faster to equilibrium. However, our method was applied to a simple model molecule (*N*,*N*-dimethylacetamide) for which one selective pulse before the recovery delay was sufficient to optimize the pulse sequence, as the non-quaternary carbons of this molecule resonate in a small window, far away from the quaternary carbon, and have similar relaxation properties. In most cases, this method will not be sufficient because the spectrum may be more complex, with a wide chemical shift range. We propose here to improve this pulse sequence so that it can be applied to various molecules, by adding a series of selective pulses before the recovery delay. This method will be applied to the molecule of vanillin, a flavouring compound widely used in food industry, for which ^{13}C NMR has been proved to be an efficient tool for origin discrimination by isotopic analysis [2].

2. Theory

2.1. General description of the magnetization time course during the recovery delay

We use the same conventions as in [12]. We first consider a simple spin system *IS* (*I*, insensitive: ^{13}C; *S*, sensitive: ^{1}H), coupled by intramolecular dipole–dipole relaxation. At the beginning of the recovery delay *T*, *I*, and *S* may both be out of equilibrium, because of the previous *S* saturation during the acquisition and because *I* may be amplified by NOE build-up.

The behaviour of *I* and *S* is described by the two differential equations, first derived by Solomon [13]:

$$\begin{aligned} \mathrm{d}\langle I_z\rangle/\mathrm{d}t &= -R_I(\langle I_z\rangle - I_0) - \sigma_{IS}(\langle S_z\rangle - S_0),\\ \mathrm{d}\langle S_z\rangle/\mathrm{d}t &= -R_S(\langle S_z\rangle - S_0) - \sigma_{SI}(\langle I_z\rangle - I_0), \end{aligned} \tag{1}$$

where I_z and S_z are the *z* components of the ^{13}C and ^{1}H magnetizations; R_I and R_S are the inverse of the carbon and ^{1}H longitudinal relaxation times, respectively. The quantities σ_{IS} and σ_{SI} are cross-relaxation terms which, in the case of two spins 1/2, are equal: $\sigma_{IS} = \sigma_{SI} = \sigma$. From these coupled equations, it is possible to find I_z magnetization at any time *t* during the delay *T*

$$\langle I_z\rangle = I_0 + C_+\exp[-\lambda_+ t] + C_-\exp[-\lambda_- t], \tag{2}$$

with

$$\lambda_\pm = 1/2\{R_I + R_S \pm [(R_S - R_I)^2 + 4\sigma^2]^{1/2}\} \tag{3}$$

and

$$C_\mp = \pm\left\{\frac{S_0\ \sigma}{\lambda_+ - \lambda_-}\right\} \pm (\langle I_z(0)\rangle - I_0)\left(\frac{\lambda_\pm - R_I}{\lambda_+ - \lambda_-}\right), \tag{4}$$

if one considers that at $t = 0$, $\langle S_z\rangle = 0$. Indeed, as *S* was saturated during all the acquisition time and its magnetization became rapidly null, it was set to zero immediately before the beginning of the recovery delay *T*.

This means that I_z goes back to equilibrium biexponentially. The relaxation rates λ_+ and λ_- are both functions of R_I, R_S, and σ, with λ_+ larger than λ_-. Therefore, the corresponding exponential term $\exp[-\lambda_+ t]$ should vanish more rapidly than $\exp[-\lambda_- t]$. Then, I_z returns to equilibrium more rapidly if $C_- \ll C_+$. In that case, equilibrium should be reached for $t = 5/\lambda_+$.

It is interesting to determine the value of $\langle I_z(0)\rangle$ for which C_- becomes null. It is called $\langle I_z(0)\rangle_{\mathrm{opt}}$

$$\langle I_z(0)\rangle_{\mathrm{opt}} = I_0 - \left(\frac{S_0\ \sigma}{\lambda_+ - R_I}\right). \tag{5}$$

The nuclear Overhauser enhancement factor η is defined by the relationship

$$\eta = \frac{S_0\sigma}{I_0 R_I}. \tag{6}$$

Then, $\langle I_z(0)\rangle_{\mathrm{opt}}$ can be written:

$$\langle I_z(0)\rangle_{\mathrm{opt}} = I_0\left(1 - \frac{R_I}{\lambda_+ - R_I}\eta\right), \tag{7}$$

$$\approx I_0\left(1 - \frac{R_I}{R_S - R_I}\eta\right). \tag{8}$$

This shows that $\langle I_z(0)\rangle_{\mathrm{opt}}$ can vary in a wide range. In most cases, it should be possible to adapt the NMR sequence so that at the beginning of the delay *T*, $\langle I_z\rangle = \langle I_z(0)\rangle_{\mathrm{opt}}$ instead of the value of $\langle I_z\rangle$ at the end of acquisition, which we call $\langle I_z\rangle_{\mathrm{AQ}}$. This would enable I_z to go back to equilibrium faster.

Globally, two different situations may occur. For quaternary carbons, the relaxation rate R_I will be very small compared to the rate λ_+, and the coefficient η will not be very large. Then, $\langle I_z(0)\rangle_{\mathrm{opt}}$ will be close to I_0. A supplementary decoupling delay should be added at the end of the acquisition to increase I_z to the expected value $\langle I_z(0)\rangle_{\mathrm{opt}}$. For other carbons, $\langle I_z(0)\rangle_{\mathrm{opt}}$ may be smaller than $\langle I_z\rangle_{\mathrm{AQ}}$. For these nuclei, I_z magnetization should be reduced at the end of the acquisition for a faster relaxation. This can be done by applying a pulse at their frequency, eventually preceded by a supplementary decoupling delay. This optimization is better performed if $\langle I_z(0)\rangle_{\mathrm{opt}}$ is known precisely.

2.2. Determination of $\langle I_z(0)\rangle_{opt}$

The exact value of $\langle I_z(0)\rangle_{\mathrm{opt}}$ can be deduced from the measurement of the Overhauser enhancement coefficient η together R_I and R_S determination by inversion–recovery [12]. The constant λ_+ can be deduced from these values via Eqs. (3) and (6). The value of $\langle I_z(0)\rangle_{\mathrm{opt}}$ is then deduced

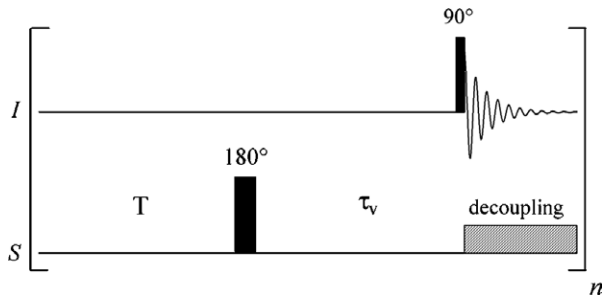

Fig. 1. Pulse sequence enabling the characterization of I_z biexponential relaxation after ^{1}H inversion. T is the recovery delay for I_z to reach its equilibrium value and τ_v is a variable delay.

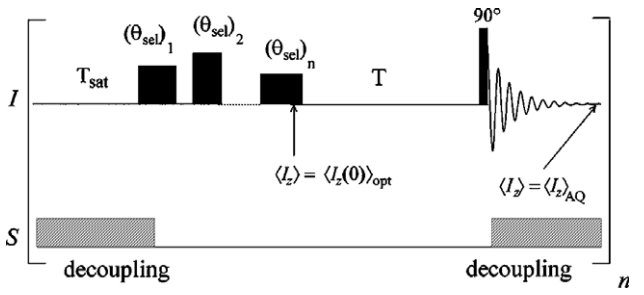

Fig. 2. Inverse-gated-decoupling sequence optimized for a faster quantification. A supplementary delay T_{sat} is added at the end of the acquisition, together with a series of selective pulses. The values of T_{sat} and θ_{sel} are adjusted so that $\langle I_z\rangle = \langle I_z(0)\rangle_{opt}$ for the different carbons at the beginning of the recovery delay T.

from Eq. (7). Though, the value found by this way is only exact at the express condition that one type of nuclei S cross-relaxes with I.

In the general case where various protons may be dipolarly coupled to I, I_z will still have approximately a biexponential behaviour and the precedent model will still be useful but λ_+ and λ_- will not depend on a given proton relaxation time in the same way. Hence, it will not be possible to determine $\langle I_z(0)\rangle_{opt}$ by this way.

Another method to determine $\langle I_z(0)\rangle_{opt}$ is to determine directly the relaxation-rate constant λ_+ while the other parameters are measured in the same way as previously. This can be done by studying I_z relaxation time course from equilibrium after S inversion. The corresponding sequence is presented in Fig. 1. During the variable delay τ_v, I_z time course is: $\langle I_z(t)\rangle = I_0 + C[(\exp(-\lambda_- \ t)) - \exp(-\lambda_+ \ t)]$ with $C = S_0\sigma/(\lambda_+ - \lambda_-)$, and a biexponential fit gives λ_+ and λ_- values. Here again, the value of $\langle I_z(0)_{opt}$ is deduced from Eq. (7).

2.3. Optimization of the sequence

Three cases can be considered. (i) If $\langle I_z\rangle_{AQ} < \langle I_z(0)\rangle_{opt} < I_0$, it is possible to saturate S during a delay T_{sat} after the acquisition until $\langle I_z\rangle = \langle I_z(0)\rangle_{opt}$. In that case, T_{sat} is adjusted so that

$$I_0(1+\eta)[1-\exp(-R_I(T_{AQ}+T_{sat}))] = \langle I_z(0)\rangle_{opt}. \quad (9)$$

(ii) If $-\langle I_z\rangle_{AQ} < \langle I_z(0)\rangle_{opt} < \langle I_z\rangle_{AQ}$, $\langle I_z\rangle$ can be reduced to the desired value by applying a RF pulse of angle θ. (iii) If $-I_0(1+\eta) < \langle I_z(0)\rangle_{opt} < -\langle I_z\rangle_{AQ}$, $\langle I_z\rangle$ can be amplified by saturating S after the acquisition until $\langle I_z = -\langle I_z(0)\rangle_{opt}$. An inversion pulse will then enable one to obtain the desired value for $\langle I_z\rangle$.

Carbons with different relaxation parameters may be present in a same sample. In that case, a global optimization can still be obtained by saturating S during a delay T_{sat} sufficient for increasing ^{13}C magnetization with the larger value of $\langle I_z(0)\rangle_{opt}$, then replacing the RF pulse of angle θ by a series of selective pulses with adequate flip angles for each carbon.

The corresponding sequence is represented Fig. 2 for different types of carbons. As in [12], the sequence consists in inverse-gated optimized decoupling, so we call it "InGOD2."

3. Materials and methods

A 3.3 mol L^{-1} aqueous solution of vanillin was obtained by dissolving 500 mg hemisynthetic vanillin, produced from lignin and obtained from Sigma–Aldrich, in 1 mL acetone-d_6. All NMR spectra were recorded at 299 K, on a Bruker Avance 400 DPX spectrometer operating at 9.4 T. ^{13}C spectra were recorded at a spectrometer frequency of 100.62 MHz with a 5 mm dual probe. Proton decoupling was obtained with the WALTZ16 mode. The standard ^{1}H decoupled ^{13}C spectrum of vanillin is represented in Fig. 3, together with the molecule of vanillin. The carbon sites were numbered in decreasing chemical shift, and the peaks attribution is the same as in [2].

Free induction decays (FIDs) were accumulated in 64K channels, with a spectral width of 20.08 kHz, an acquisition time of 1.63 s, using 90° read pulses of duration 6.7 μs, and 32 transients.

An exponential apodisation function of 5.0 Hz was applied to the FID prior to Fourier transformation.

Longitudinal relaxation times of ^{13}C were determined by using an inversion–recovery sequence with the decoupler on continuously. An inversion–recovery sequence was employed for ^{1}H longitudinal relaxation times determination. The baseline was corrected automatically and the areas of the peaks were analysed within the Bruker software.

Nuclear Overhauser enhancement factors (η) for the different carbon sites were obtained by comparison of the corresponding peak areas I_{sat} and I_0 determined by Lorentzian deconvolution when ^{1}H were decoupled and inverse-gated decoupled, respectively [4], waiting 240 s between the end of the acquisition and the read pulse. They are defined as: $I_{sat}/I_0 = 1+\eta$.

The relaxation rate constants λ_+ and λ_- of the ^{13}C were determined by studying the transient state of ^{13}C magnetization after a ^{1}H inversion by a 180° pulse of duration 19.4 μs applied at ^{1}H frequency. These values could be obtained via the pulse sequence described in Fig. 1. There,

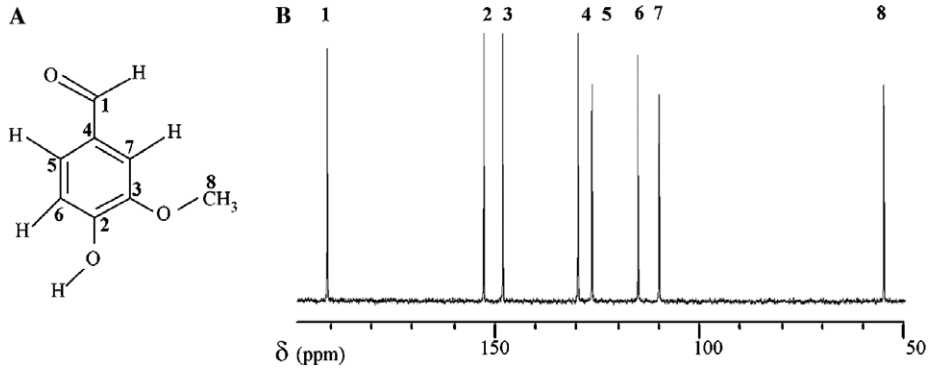

Fig. 3. Vanillin molecule with carbon sites numbered in decreasing chemical shift (A) and ^{13}C NMR spectrum of vanillin recorded at 299 K, in a 9.4 T spectrometer with 32 transients (B).

the relaxing delay T should be sufficient for all quaternary carbons to go back to equilibrium, that means 7 T_{1max}, and would be followed by a ^{1}H inverting pulse and a variable delay τ_v between 3 μs and 100 s. Preliminary relaxation measurement showed us that the delay T necessary for such an experiment would be about 184 s and hence, the experimental time would be very long. Experiments performed in [12] showed us that the relaxation of quaternary carbons was faster when a ^{1}H saturating delay T_{sat} setting ^{13}C longitudinal magnetization to $\langle I_z(0)\rangle_{opt}$ was included between the end of the acquisition and the beginning of the recovery delay. Measurements of ^{13}C and ^{1}H longitudinal relaxation times, together with the NOE enhancement coefficient η, enabled us to estimate approximately $\langle I_z(0)\rangle_{opt}$. It was equal to 0.73, 0.89, and 0.82 for C-2, C-3, and C-4, respectively. Hence, after a saturation delay of 10 s, the intensities of the carbons C-2, C-3, and C-4 were, respectively, 0.99, 0.66, and 0.91. As C-3 relaxes the slower, we consider it is sufficient that it relaxes for all carbons to go back to equilibrium. Its magnetization is lower than $\langle I_z(0)\rangle_{opt}$. Then, it should go back to equilibrium almost as fast as if it would relax exponentially with the relaxation rate T_1(C-3). Then, a delay T of 50 s after the saturation delay of 10 s should be sufficient for all carbons to go back to equilibrium. This calculation enables us to do the corresponding experiment significantly faster. It is not very precise but even if magnetization was not gone to equilibrium at the beginning of the variable delay τ_v, the constants λ_+ and λ_- could still be measured. Their values would only be less precise.

Phase and baseline were corrected manually. For each carbon, the evolution of the intensity was determined by peak picking. Biexponential curves were adjusted to the corresponding data via a least-square fit to determine the relaxation rate constants λ_+ and λ_-.

The recovery of the ^{13}C magnetization was studied by applying either an inverse-gated-decoupling sequence or the optimized sequence (Fig. 2) and waiting delays from 3 μs to 240 s between the end of the decoupling delay and the read pulse. The optimized sequence was obtained by applying a saturating delay T_{sat} of either 0.7 s, 9 s, or 12 s eventually followed by a series of low-power-rectangular pulses centred at the desired frequencies and then the recovery delay from 3 μs to 240 s. The duration, power, applied frequency, and rotating angle of the low power pulses are given in Table 1. The spectra were analysed in the same way as for the experiment where the relaxation rate constants λ_+ and λ_- were determined.

Table 1
Properties of the selective pulses applied successively during the optimized inverse-gated-decoupling sequence, with a saturation delay of 12 s (a) or 0.7 s (b)

Carbon	Pulse duration (ms)	Pulse power attenuation (dB)	Applied frequency (kHz)	Rotating angle (degrees)
(a)				
C-2	1.740	54	4.8	54
C-4	0.650	46	2.5	24
(b)				
C-1	1.670	46	8.7	125
C-5	4.270	54	2.2	128
C-6 and C-7	1.280	42	0.8	150
C-8	2.356	46	−4.9	177

Measurements were performed at 299 K, in a 9.4 T spectrometer. The pulse power attenuation was compared to the read pulse power. The applied frequency was measured relative to the central frequency of the spectrum at 105 ppm.

4. Results and discussion

At the temperature considered, vanillin is composed of 1 CH_3 group, 4 non-equivalent CH, and of 3 quaternary carbons, as shown in Fig. 3. The measured relaxation times of vanillin are given in Table 2, together with the nuclear Overhauser enhancement η at steady state while ^{1}H were saturated. For each carbon, the longitudinal relaxation time of the closer ^{1}H group was also reported. The measured ^{1}H relaxation times correspond to ^{1}H bonded in majority to ^{12}C, whereas those bonded to ^{13}C would interest us. We neglect the difference between these values. The coefficient $\langle I_z(0)\rangle_{opt}$ was calculated in two ways. It was first deduced from $T_1(^{13}C)$, $T_1(^{1}H)$ and η via Eqs. (3), (6), and (7). The result, normalized to I_0, is represented in Table 2,

Table 2
Relaxation properties for the different carbons and for the protons dipolarly coupled to them

Carbon	$T_1(^{13}C)$ (s)	$T_1(^1H)$ (s)	η	$\frac{\langle I_z(0)\rangle_{opt}}{I_0}$ (a)	$\lambda_+(s^{-1})$	$\frac{\langle I_z(0)\rangle_{opt}}{I_0}$ (b)
C-1	2.76	3.53	1.71	−4.12	0.79	−0.89
C-2	17.0	3.69	1.00	0.72	0.22	0.65
C-3	26.3	3.02	0.86	0.89	0.34	0.89
C-4	16.7	3.02	0.81	0.82	0.43	0.87
C-5	1.97	3.05	1.82	−4.81	0.74	−1.21
C-6	2.25	3.69	1.92	−4.90	0.77	−1.80
C-7	2.25	3.02	1.94	−4.15	0.75	−1.49
C-8	2.77	1.81	1.99	−1.39	0.72	−1.70

Measurements were performed at 299 K, in a 9.4 T spectrometer. The acquisition time was 1.63 s. The optimal value $\langle I_z(0)\rangle_{opt}$ was deduced from the relaxation parameters $T_1(^{13}C)$, $T_1(^1H)$, and η (a), and from $T_1(^{13}C)$, λ_+, and η (b).

column (a). $\langle I_z(0)\rangle_{opt}$ was also deduced from λ_+ measurement via Eq. (7). The corresponding result is also represented in Table 2, column (b).

One observes important differences for $\langle I_z(0)\rangle_{opt}$ calculated via the two methods, particularly for carbons C-1, C-5, C-6, and C-7. More than one group of ^1H may interact with these carbons. There, the method (a) should be less appropriate that the method (b) where λ_+ is measured directly. Then, we will consider the method (b) gives the expected value. In the presence of non-quaternary carbons close to more than one ^1H group, it is important to use the method (b) even though the preliminary optimization is then longer. For quaternary carbons, parameters obtained via the method (a) are less precise but they should be useful each time a faster return to equilibrium is needed and there is not much time for preliminary optimization measurements. We performed simulations of C-2, C-3, and C-4 where the saturation delay before the recovery delay T was either deduced from ^1H and ^{13}C longitudinal relaxation times (method (a)), and λ_+, $T_1(^{13}C)$ (method (b)). These simulations were performed with the program Microsoft Excel 2003. The magnetization time course of each carbon during the recovery delay T was modelized as a biexponential with the relaxation rates λ_+ and λ_- measured experimentally. We then determined the delay T necessary for a recovery of the corresponding magnetization at 1% (Table 3). For a comparison, the recovery of quaternary carbons was also simulated after an inverse-gated decoupling sequence with an acquisition time of 1.63 s and after a saturation delay T_{sat} setting I_z to I_0. Here again, the delay necessary for a recovery at 1% was determined.

One observes that for a carbon with a very long T_1, as C-3, it is not necessary to measure λ_+ for a good optimization; an approximate value deduced from ^1H and ^{13}C longitudinal relaxation times gives a quite well-optimized sequence. As a matter of fact, for the other carbons whose magnetization biexponential behaviour is more pronounced, the global time necessary for magnetization recovery will become significantly longer with the method (a) compared to the method (b). But whatever the method for determining $\langle I_z(0)\rangle_{opt}$, the sequence will be significantly time-saving compared to the standard inverse-gated-decoupling sequence. The sequence obtained this way is also far more efficient that if ^{13}C magnetization was set to I_0 by a long enough ^1H saturating delay T_{sat} at the beginning of the recovery delay T. This is because in this last case, as ^1H are out of equilibrium, ^{13}C magnetization will be amplified. One should note that in certain cases, herein for carbons C-3 and C-4, setting I_z to I_0 at the beginning of the recovery delay gives worse results than the standard inverse-gated-decoupling sequence.

In the same way, if one wants to study a sample in different conditions, changing its temperature and/or concentration, the longitudinal relaxation times may be modified. Then, the coefficient $\langle I_z(0)\rangle_{opt}$ and hence the saturating delay T_{sat}, deduced from an initial measurement, may differ from the effective optimal value. We performed simulations where the initial saturation delay was inadequate, due to over- or underestimation of the relaxation times of 10%. Then, the calculated value of T_{sat} was modified. As in the previous simulations, we determined for each carbon the time necessary for a recovery at 1%. The result is presented in Table 4. One observes that the recovery is longer than when the sequence is well optimized. But it is still significantly faster than in the standard inverse-gated-decoupling sequence. For larger fluctuations of the relaxation parameters, optimization of the sequence may be necessary again.

Table 3
Calculation for various acquisition parameters of the delays necessary for the magnetization recovery to I_0 with a 1% precision

Carbon	Global recovery delay (s) with a 1% precision			
	Inverse-gated-decoupling	Optimization method (a)	Optimization method (b)	Sequence where $\langle I_z(0)\rangle_{sat} = I_0$
C-2	62.8	39.9	22.6	**68.4**
C-3	62.7	24.9	**24.2**	54.4
C-4	**85.7**	**40.4**	16.9	64.3

Global recovery delays include the acquisition time, the saturating delay T_{sat} and the recovery delay T described in Fig. 2. The hypothesis were that for each carbon C-i, $\langle I_z\rangle$ relaxes exponentially during $T_{AQ} + T_{sat}$, with the measured relaxation time T_1(C-i), and relaxes biexponentially during the delay T, from $\langle I_z(0)\rangle_{sat}$ to I_0, with the measured relaxation rates λ_+ and λ_-. In each simulation, the delay T_{sat} was adjusted for $\langle I_z(0)\rangle_{sat}$ to be set to the expected value. Both optimization procedures (method (a), using $T_1(^{13}C)$ and $T_1(^1H)$ and method (b), using $T_1(^{13}C)$ and λ_+) are compared to the inverse-gated-decoupling sequence and to the sequence where $\langle I_z(0)\rangle_{sat}$ was set to I_0. In each case, the duration of the sequence necessary for a global relaxation is given by the carbon which has the slower magnetization recovery (printed in bold).

Table 4
Calculation of the delays necessary for the magnetization recovery to I_0 with a 1% precision when the relaxation parameters are badly estimated

Carbon	Global recovery delay (s) with a 1% precision		
	Optimization method (b)	Overestimation of 10% of the relaxation times	Underestimation of 10% of the relaxation times
C-2	22.6	31.5	34.0
C-3	**24.2**	45.2	42.8
C-4	16.9	**47.1**	**46.2**

Simulations were performed in the same way as in Table 3. The bad estimation of the relaxation parameters modified the expected value of T_{sat} and hence $\langle I_z(0)\rangle_{sat}$ and the delay T. In each case, the duration of the sequence necessary for a global relaxation is given by the carbon that has the slower magnetization recovery (printed in bold).

Here again, if the optimization needs to be done rapidly, the measurement of $T_1(^{13}C)$, $T_1(^1H)$, and η will be sufficient.

All these simulations show us that for quaternary carbons the choice of an initial saturation delay T_{sat}, deduced from preliminary optimization measurements, enables a faster return to equilibrium than with the standard inverse-gated-decoupling sequence. It also shows that the preliminary optimization measurements can be shorten if necessary. We will now check whether similar results are obtained experimentally.

The value of $\langle I_z\rangle$ at the end of the acquisition, called $\langle I_z\rangle_{AQ}$, was measured by applying an inverse-gated-decoupling sequence where the delay T is null. It is reported in Table 5 for quaternary carbons C-2, C-3, and C-4. For these carbons, a supplementary saturating delay T_{sat} at the end of the acquisition accelerates their relaxation during the delay T. The optimal value of T_{sat} was deduced from Eq. (9) and is also reported in Table 5. One observes that the optimal value of T_{sat} is very different for C-2, C-3, and C-4. We simulated these carbons time course via Eqs. (2)–(4) and (6) after different saturating delays T_{sat}. These simulations show that the optimal delay T_{sat} for a global faster relaxation is $T_{sat} = 9$ s.

We decided first to detect all carbons previously enhanced during a delay T_{sat} of 9 s. The result of this experiment was compared to a simple inverse-gated-decoupling sequence. For the quaternary carbons C-2 to C-4, the sequence where a saturation delay of 9 s is added at the beginning of the recovering delay is slightly better than the standard inverse-gated-decoupling sequence, even though all non-quaternary carbons go back to equilibrium in a longer time. The global return to equilibrium is still limited by the quaternary carbons.

Then, we decided to focalize our attention on quaternary carbons relaxation. We added a decoupling delay T_{sat} of 12 s after acquisition to allow C-3 magnetization to reach its optimum value. For C-2 and C-4, I_z magnetization at the end of this delay was estimated via the equation

$$\langle I_z(0)\rangle_{sat} = I_0(1+\eta)[1-\exp(-R_I(T_{AQ}+T_{sat}))]. \quad (10)$$

Then, the magnetization of the carbons C-2 and C-4 along z axis was reduced by applying a selective pulse θ_{opt} deduced from the equation:

$$\cos(\theta_{opt}) = \left(\frac{\langle I_z(0)\rangle_{opt}}{\langle I_z(0)\rangle_{sat}}\right), \quad (11)$$

where $\langle I_z(0)\rangle_{opt}$ is the value written in Table 2, column (b).

The corresponding values are given in Table 6. We applied selective pulses on C-2 and C-4 to reduce their magnetization at the end of the saturating delay. Their properties are given in Table 1, column (a).

The result of this experiment was compared to the inverse-gated-decoupling sequence. The ^{13}C magnetization time course of C-3 is represented in Fig. 4 as a function of T for the optimized pulse sequence (■), for the standard inverse-gated-decoupling sequence (○), and for the sequence where a T_{sat} delay of 9 s is added (△). The delay necessary for each carbon magnetization to go back to equilibrium is given in Table 7. One observes that quaternary carbons magnetization recovers faster when the optimized sequence with a delay T_{sat} of 12 s is employed. One can notice that the relaxation of non-quaternary carbons is still faster than those of the quaternary carbons, even if no selective pulse is applied on them. Globally, the duration of the optimized sequence is divided by two compared to the usual inverse-gated-decoupling sequence.

Finally, in the present case, optimization of quaternary carbons relaxation is sufficient to shorten the recovery delay as much as possible. A similar result should be obtained each time few carbons relax significantly slower than the others.

Table 5
Longitudinal magnetization at the end of the acquisition for each quaternary carbon of vanillin during the inverse-gated-decoupling sequence

Carbon	$\langle I_z\rangle_{AQ}/I_0$	$(T_{sat})_{opt}$ (s)
C-2	0.18	4.92
C-3	0.11	15.6
C-4	0.17	9.32

Measurements were performed at 299 K, in a 9.4 T spectrometer. The acquisition time was 1.63 s. The normalized value $\langle I_z\rangle_{AQ}/I_0$ is reported together with the optimal saturation delay $(T_{sat})_{opt}$ for a faster magnetization recovery.

Table 6
Determination of the optimal rotating angle θ_{opt} for a faster recovery of quaternary carbons of vanillin after a 12 s saturation delay

Carbon	$\langle I_z\rangle_{AQ}/I_0$	$\langle I_z(0)\rangle_{sat}/I_0$	θ_{opt} (degrees)
C-2	0.18	1.10	53.91
C-3	0.11	0.75	—
C-4	0.17	0.85	24.43

Measurements were performed at 299 K, in a 9.4 T spectrometer. The acquisition time was 1.63 s. The normalized value $\langle I_z\rangle_{AQ}/I_0$ is reported together with $\langle I_z(0)\rangle_{sat}/I_0$, the normalized magnetization at the end of the saturating delay T_{sat} and θ_{opt} the optimal rotating angle after a saturating delay $T_{sat} = 12$ s.

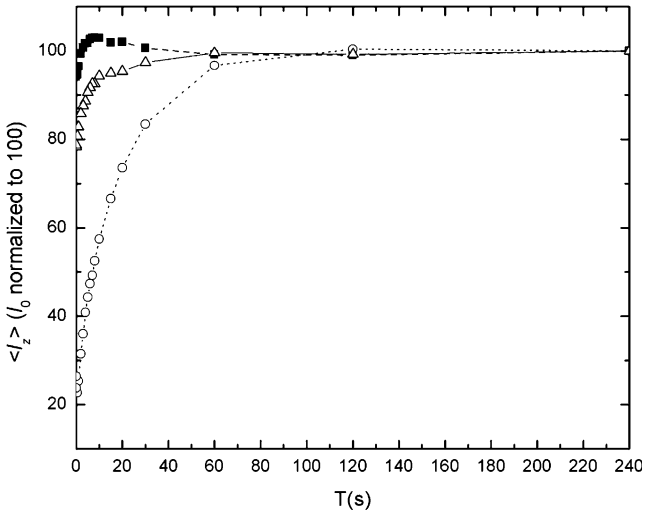

Fig. 4. ^{13}C longitudinal magnetization time course as a function of the recovery delay T, for C-3. The signal detected after the optimized sequence ($T_{sat} = 12$ s and selective pulses applied on C-2 and C-4) (■) is compared to those detected after the standard inverse-gated-decoupling sequence (○), and after a sequence where only a saturation delay of 9 s is added (△).

Table 7
Global recovery delays (including the acquisition time) of vanillin ^{13}C magnetization for which $\langle I_z \rangle = I_0$ with a 2% precision

Carbon	Global recovery delay (s)	
	Inverse-gated-decoupling	Optimized sequence
C-1	14.8	25.8
C-2	45.7	**34.9**
C-3	**69.8**	33.9
C-4	47.1	17.6
C-5	10.1	21.6
C-6	13.3	24.8
C-7	13.2	24.1
C-8	13.8	27.3

Comparison between the inverse-gated-decoupling sequence and the optimized sequence with $T_{sat} = 12$ s and selective pulses applied on quaternary carbons. In each case, the duration of the sequence necessary for a global relaxation is given by the carbon which has the slower magnetization recovery (printed in bold).

Some samples may exist, where various carbons are present, but without any quaternary carbon with a much longer longitudinal relaxation time. Then, we decided to optimize the sequence for the same sample, considering non-quaternary carbons only. All ^{13}C magnetization was enhanced during a delay T_{sat} of 0.7 s. For each carbon, I_z magnetization at the end of the saturating delay was calculated via Eq. (10). Then, θ_{opt} was deduced from Eq. (11) for the different carbons, where $\langle I_z(0) \rangle_{opt}$ is the value written in Table 2, column (b).

The calculated values of $\langle I_z(0) \rangle_{sat}$ and θ_{opt} are represented in Table 8 for each carbon.

From these theoretical values, we decided to apply selective pulses on C-1, C-5, C-8, and on the middle of C-6 and C-7. All their properties are given in Table 1, column (b). By this way, the ^{13}C magnetization of the non-quaternary

Table 8
Determination of the optimal rotating angle θ_{opt} for a faster recovery of non-quaternary carbons of vanillin after a 0.7 s saturation delay

Carbon	$\langle I_z \rangle_{AQ}/I_0$	$\langle I_z(0) \rangle_{sat}/I_0$	θ_{opt} (degrees)
C-1	1.21	2.33	112.4
C-5	1.59	1.98	127.7
C-6	1.50	1.91	160.5
C-7	1.52	1.93	140.5
C-8	1.33	1.73	169.3

Measurements were performed at 299 K, in a 9.4 T spectrometer. The acquisition time was 1.63 s. The normalized value $\langle I_z \rangle_{AQ}/I_0$ is reported together with $\langle I_z(0) \rangle_{sat}/I_0$, the normalized magnetization at the end of the saturating delay T_{sat} and θ_{opt} the optimal rotating angle after a saturating delay $T_{sat} = 0.7$ s.

carbons was significantly reduced before the evolution delay T.

The result of this experiment was compared to a simple inverse-gated-decoupling sequence. Fig. 5 represents, for C-5, ^{13}C magnetization time course as a function of T for the optimized pulse sequence (■) compared to the inverse-gated-decoupling sequence (○). For comparison, a simulation of C-5 magnetization recovery from I_0 is also reported (–). It would correspond to the signal detected with a selective pulse setting I_z to I_0 at the beginning of the recovery delay T. One observes as expected that the choice of $\langle I_z(0) \rangle_{opt}$ as initial magnetization leads to a faster return to equilibrium for the optimized sequence than for the other ones.

So as to compare the efficiency of the optimized and the inverse-gated-decoupling sequences for the non-quaternary carbons, we determined for each one the delay necessary for the return to equilibrium after the read pulse, with a

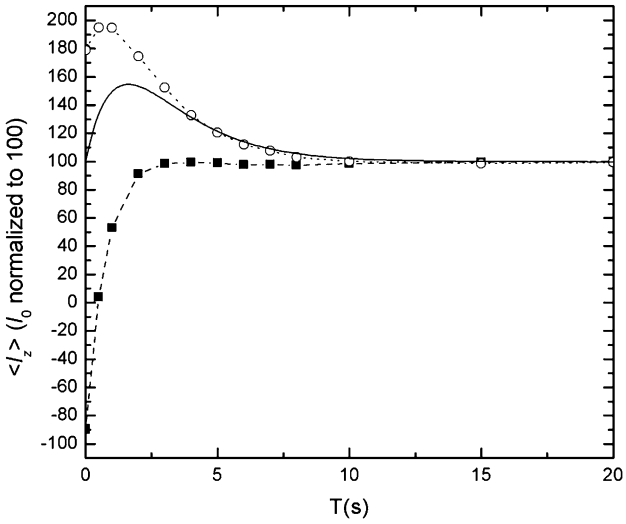

Fig. 5. ^{13}C longitudinal magnetization time course as a function of the recovery delay T, for C-5. The signal detected after the optimized sequence ($T_{sat} = 0.7$ s and selective pulses applied on non-quaternary carbons) (■) is compared to those detected after the standard inverse-gated-decoupling sequence (○), and to a simulation where a signal with similar relaxation properties in initially set to I_0 (—).

Table 9
Global recovery delays (including the acquisition time) of vanillin ^{13}C magnetization for which $\langle I_z \rangle = I_0$ with a 2% precision.

Carbon	Global recovery delay (s)	
	Inverse-gated-decoupling	$T_{sat} = 0.7$ s and selective pulses
C-1	**14.8**	9.2
C-5	10.1	**11.3**
C-6	13.3	8.7
C-7	13.2	7.9
C-8	13.8	10.5

Comparison between the inverse-gated-decoupling sequence and the optimized sequence with $T_{sat} = 0.7$ s, with selective pulses applied on non-quaternary carbons. In each case, the duration of the sequence necessary for a global relaxation is given by the carbon which has the slower magnetization recovery (printed in bold).

precision of 2%. The corresponding delays are given, for each sequence, in Table 9. For each sequence, the delay necessary for all carbons to go back to equilibrium is printed in bold.

One observes that the optimized sequence can be performed in about 24% less time than the inverse-gated-decoupling sequence. Though, the saving of time is much less interesting than in the presence of quaternary carbons.

5. Conclusion

We have shown that the inverse-gated-decoupling sequence can be improved for quantitative analysis in a shorter time even in a molecule with carbons of various relaxation properties in a large spectral range. If all the carbons of interest have short relaxation times and a large value of η, applying a series of selective pulses, eventually preceded by a saturation delay, after the acquisition time, can accelerate the recovery of their magnetization. In the presence of quaternary ^{13}C with various relaxation times and short η factor, this result can be obtained by applying at the beginning of the recovery delay, a saturation delay where the carbons magnetization will be increased by nuclear Overhauser enhancement, followed by a series of selective pulses that diminish the magnetization of some carbons too amplified. The optimal longitudinal magnetization for each carbon can be deduced precisely from its NOE enhancement at steady state, its longitudinal relaxation time, together with the determination of the larger longitudinal relaxation rate constant λ_+ depending on ^1H nuclei dipolarly coupled to it.

The method is particularly efficient for a sample containing quaternary carbons that relax very slowly. For the vanillin sample that we studied, the application of a saturation delay divided by 2 the recovery time of the slower quaternary carbon. Two selective pulses applied on the other quaternary carbons were then sufficient for a global acceleration of relaxation.

Even if considerable time is necessary for the sequence optimization, it will still be useful when a large number of experiments are required on similar samples, as for the determination of natural-compounds origin. For alike samples where the relaxation times fluctuate in a 10% range, the precedent optimization is less efficient but it still gives better results than the inverse-gated-decoupling sequence. Also, when a less precise optimization is needed, the only measurement of ^1H and ^{13}C longitudinal relaxation times, together with the NOE enhancement factor η, will still enable a saving of time compared to the standard inverse-gated-decoupling sequence.

This method was tested by ^{13}C NMR but it may be applied on any other nuclei dipolarly coupled to ^1H. It may be developed in many fields where precise quantitative NMR is needed despite the presence of dipolar couplings.

References

[1] T. Mavromoustakos, M. Zervou, E. Theodropoulou, D. Panagiotopoulos, G. Bonas, M. Day, ^{13}C NMR analysis of the triacylglycerol composition of Greek virgin olive oils, Magn. Reson. Chem. 35 (1997) S3–S7.
[2] E. Tenailleau, P. Lancelin, R.J. Robins, S. Akoka, NMR approach to the quantification of nonstatistical ^{13}C distribution in natural products: vanillin, Anal. Chem. 76 (2004) 3818–3825.
[3] M. Aursand, L. Jorgensen, H. Grasdalen, Quantitative high-resolution ^{13}C Nuclear Magnetic Resonance of anserine and lactate in white muscle of Atlantic salmon (*Salmo salar*), Comp. Biochem. Physiol. 112B (1995) 315–321.
[4] R. Freeman, H.D.W. Hill, R. Kaptein, Proton-decoupled NMR spectra of carbon-13 with the nuclear Overhauser effect suppressed, J. Magn. Reson. 7 (1972) 327–329.
[5] D. Canet, Systematic errors due to improper waiting times in heteronuclear Overhauser effect measurements by the gated decoupling technique, J. Magn. Reson. 23 (1976) 361–364.
[6] R.K. Harris, R.H. Newman, Choice of pulse spacings for accurate T_1 and NOE measurements in NMR spectroscopy, J. Magn. Reson. 23 (1976) 449–456.
[7] S.J. Opella, D.J. Nelson, O. Jardetzky, Dynamics of nuclear Overhauser enhancement in proton decoupled carbon-13 nuclear magnetic resonance, J. Chem. Phys. 64 (1976) 2533–2535.
[8] J.N. Shoolery, Some quantitative applications of ^{13}C NMR spectroscopy, Prog. NMR Spectrosc. 11 (1977) 79–93.
[9] E. Baguet, T. Magot, K. Ouguerram, R.J. Robins, R. Weesie, Simultaneous quantification of free and esterified cholesterol extracted from plasma by ^{13}C NMR spectroscopy, Analusis 27 (1999) 876–881.
[10] D.M. Doddrell, D.T. Pegg, M.R. Bendall, Distortionless enhancement of NMR signals by polarization transfer, J. Magn. Reson. 48 (1982) 323–327.
[11] N. Karabulut, E. Baguet, M. Trierweiler, S. Akoka, Improvement in quantitative accuracy of ^{13}C DEPT integrals by parameter-optimization, Anal. Lett. 34 (2002) 2549–2563.
[12] P. Giraudeau, J.L. Wang, E. Baguet, Improvement of the inverse-gated decoupling sequence for a faster quantitative analysis by ^{13}C NMR, C. R. Chim. 9 (2006), in press.
[13] I. Solomon, Relaxation processes in a system of two spins, Phys. Rev. 99 (1955) 559–565.